Electronic Supporting Information

High performance hybrid white and multi-colour electroluminescence from a new host material for heteroleptic naphthyridinolate platinum complex dopant

Anurach Poloek,[abc] Chin-Ti Chen,*[a] and Chao-Tsen Chen*[c]

[a] *Institute of Chemistry, Academia Sinica, Taipei, Taiwan 11529, Republic of China, E-mail: chintchen@gate.sinica.edu.tw Fax: +886-2-27831237; Tel:+886-2-2788542*
[b]*Nano Science and Technology Program, TIGP, Acedemia Sinica, Taipei, Taiwan 11529, Republic of China*
[c] *Department of Chemistry, National Taiwan University, Taipei, Taiwan 10617, Republic of China*

General information of experimental

Photoluminescence (PL) spectra were recorded on a Hitachi fluorescence spectrophotometer F-4500, and the same spectrophotometer was used to record the EL spectra of OLEDs. UV-visible absorption spectra were recorded on a Hewlett-Packard 8453 Diode Array spectrophotometer. The ^{1}H and ^{13}C NMR spectra were recorded on a Bruker AMX-400 MHz or AVA-400 MHz Fourier-transform spectrometer at room temperature. Elemental analyses (on a Perkin-Elmer 2400 CHN
Elemental Analyzer) and electrospray ionization (ESI) or matrix-assisted laser desorption/ionization time-of-flight (MALDI-TOF) mass spectra (on a VA Analytical 11-250J or 4800 MALDI TOF/TOF Analyzer) were recorded by the Elemental Analyses and Mass Spectroscopic Laboratory in-house service of the Institute of Chemistry, Academic Sinica. Thermogravimetric analyses were performed under nitrogen with a Perkin-Elmer TGA-7 TG analyzer. Luminescence lifetime was determined on an Edinburgh FL920 time-correlated pulsed single-photon-counting instrument. Electrochemical redox potentials of the compounds were determined by cyclic voltammetry (CV) using a BAS 100B electrochemical analyzer with a scanning rate at 100 mV/s. The interested compounds were dissolved in deoxygenated dry CH_2Cl_2 with 0.1 M tetrabutylammonium perchlorate as the electrolyte. We used a platinum working electrode and a saturated nonaqueous $Ag/AgNO_3$ referenced electrode. Ferrocene was used for potential calibration (all reported potentials are referenced against Ag/Ag+) and for reversibility criteria.

Materials

For the materials used in device fabrication, NPB,[1] CBP,[2] TPBI,[3] 2-(2,4-difluorophenyl)pyridine (**F**)[4] and 4-hydroxy-8-methyl-1,5-napthyridine (**mND**)[5] were prepared via published methods. 4P-NPD was synthesized by Suzuki cross coupling reaction of N-(4-bromophenyl)-N-phenylnaphthalen-1-amine (**1**)[6] and 4,4'-biphenyldiboronic acid (**2**)[7]. Both precursors (**1** and **2**) were prepared according to the procedure described in the literatures. Synthesis detail of **4P-NPD** is given below. All materials used in OLED fabrication were purified by vacuum train sublimation prior to use.

OLED device fabrication and measurements

OLED devices were fabricated by thermal vacuum deposition. The substrate was an indium-tin-oxide (ITO) coated glass (Merck Display Technology, Taiwan) with a sheet resistance of <50 Ω/sq. ITO-coated glass substrates were cleaned with detergent, deionized water, acetone, and isopropanol, followed by oxygen plasma treatment. The current density–voltage–luminance characteristics of the devices were measured using a Keithley 2400 source meter and a Newport 1835C optical meter equipped with a Newport 818-ST silicon photodiode, respectively. The device was placed close to the photodiode such that all the forward light entered the photodiode. The effective size of the emitting diodes was 4.00 mm^2, which is significantly smaller than the active area of the photodiode detector, a condition known as "under-fillling", satisfying the measurement protocol.[8] This is one of the most conventional ways in measuring the EL efficiency of OLEDs, although sometimes experimental errors may arise due to the non-Lambertian emission of OLEDs. The color rendering index (CRI) of white OLEDs was measured by a spectroradiometer (Specbos 1201, JETI Technishe Instrumente GmbH).

Synthesis procedure

Synthesis of **FPtmND**

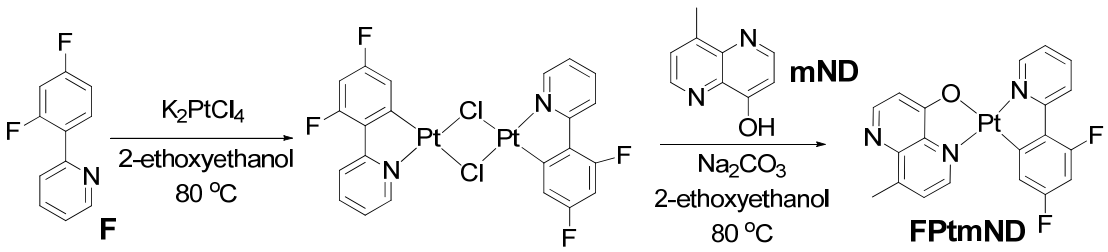

The Pt μ-dichloro-bridged dimers were prepared following literature procedures.[9] The K_2PtCl_4 and 2.5 equivalent of 2-(2,4-difluorophenyl)pyridine (**F**) ligands were

mixed in a 3:1 mixture of 2-ethoxyethanol and water. The mixture was heated to 80 °C for 16 h. The Pt-dimer was precipitated in water. The resulting yellow-greenish powder was filtered and was subsequently reacted with 4-hydroxy-8-methyl-1,5-napthyridine (**mND**) ligand without further purification.

A stirred mixture of Pt-dimer (0.150 g, 0.18 mmol), Na_2CO_3 (0.189 g, 1.80 mmol) and **mND** (0.060 g, 0.38 mmol) in 2-ethoxyethanol (25 mL) was heated to 80 °C for 16 h. After cooling the mixture to room temperature, the solution was concentrated under reduced pressure. The resulting residue was subjected to column chromatography (silica gel, CH_2Cl_2/MeOH 15:1(v/v)) to give product as a red solid in 0.150 g (77% yields). ^{1}H NMR (400 MHz, CD_3Cl): δ 9.23 (d, 1H, J = 5.6 Hz), 8.74 (d, 1H, J = 5.20 Hz), 8.48 (d, 1H, J = 5.20 Hz), 7.93 (d, 1H, J = 7.60 Hz), 7.84 (t, 1H, J = 7.60 Hz), 7.43 (d, 1H, J = 4.80 Hz), 7.14 (d, 1H, J = 6.00 Hz), 6.90 (d, 1H, J = 9.20 Hz), 6.80 (d, 1H, J = 5.20 Hz), 6.61 (t, 1H, J = 9.80 Hz), 2.78 (s, 3H). ^{13}C NMR (100 MHz, CD_3Cl): δ 173.74, 153.33, 151.37, 149.42, 146.12, 145.89, 145.61, 142.16, 139.19, 124.34, 122.02, 121.82, 121.47, 114.17, 144.14, 112.46, 99.70, 99.44, 99.17, 18.03. HR-ESI-MS: calcd. 544.07, *m/z* = 544.07 (M^+). Anal. Found (calcd) for $C_{20}H_{13}F_2N_3OPt$: C 44.29 (44.12), H 2.42 (2.41), N 7.54 (7.72).

Synthesis of **4P-NPD**

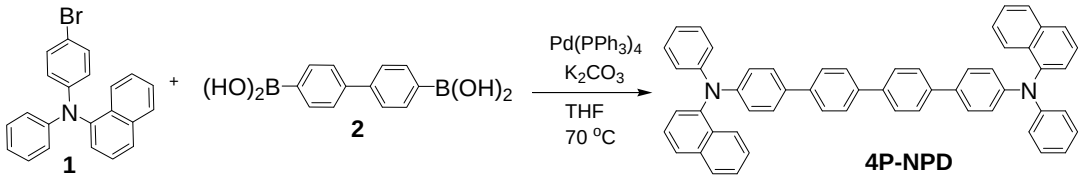

N-(4-bromophenyl)-N-phenylnaphthalen-1-amine (**1**) (2.00 g, 5.36 mmol), 4,4'-biphenyldiboronic acid (**2**) (0.62 g, 2.56 mmol) and tetrakis(triphenylphosphine)palladium(0) (0.15 g, 0.13 mmol) were dissolved in 50 mL of THF. After 30 mL of aqueous 2N K_2CO_3 was delivered, reaction mixture was heated at 70 °C for 14 h. The cooled crude mixture was poured onto water and extracted with CH_2Cl_2 (100 mL × 3) then dried over anhydrous magnesium sulfate. The product was purified over silica gel using hexane as the eluent. **4P-NPD** was obtained as a white powder (1.03 g, 54%). ^{1}H NMR (400 MHz, CD_3Cl): δ 7.97 (d, 2H, J = 8.40 Hz), 7.89 (d, 2H, J = 8.40 Hz), 7.79 (d, 2H, J = 8.40 Hz), 7.68-7.59 (m, 8H), 7.50-7.43 (m, 8H), 7.38-7.34 (m, 4H), 7.23 (t, 4H, J = 7.8 Hz), 7.10 (t, 8H, J = 8.20 Hz), 6.97 (t, 2H, J = 7.20 Hz). ^{13}C NMR (100 MHz, CD_3Cl): δ 148.20, 147.92, 143.39, 139.57, 138.93, 135.34, 133.53, 131.31, 129.16, 128.42, 127.52, 127.32, 127.19, 126.87, 126.37, 126.18, 124.26, 122.25, 122.01, 121.65. HR-(MALDI-TOF)-MS: calcd. 740.32, *m/z* = 740.32 (M^+). Anal. Found (calcd) for $C_{56}H_{40}N_2$: C 90.60 (90.78), H 5.35 (5.44), N 3.60 (3.78).

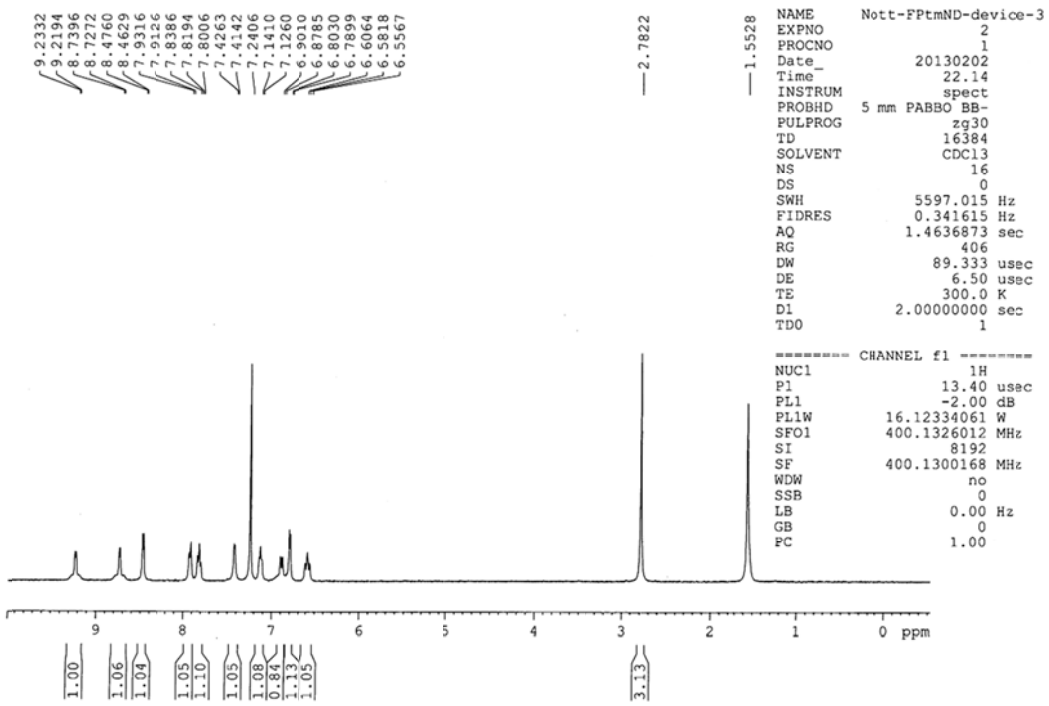

Figure S1 ^{1}H NMR spectrum of **FPtmND**.

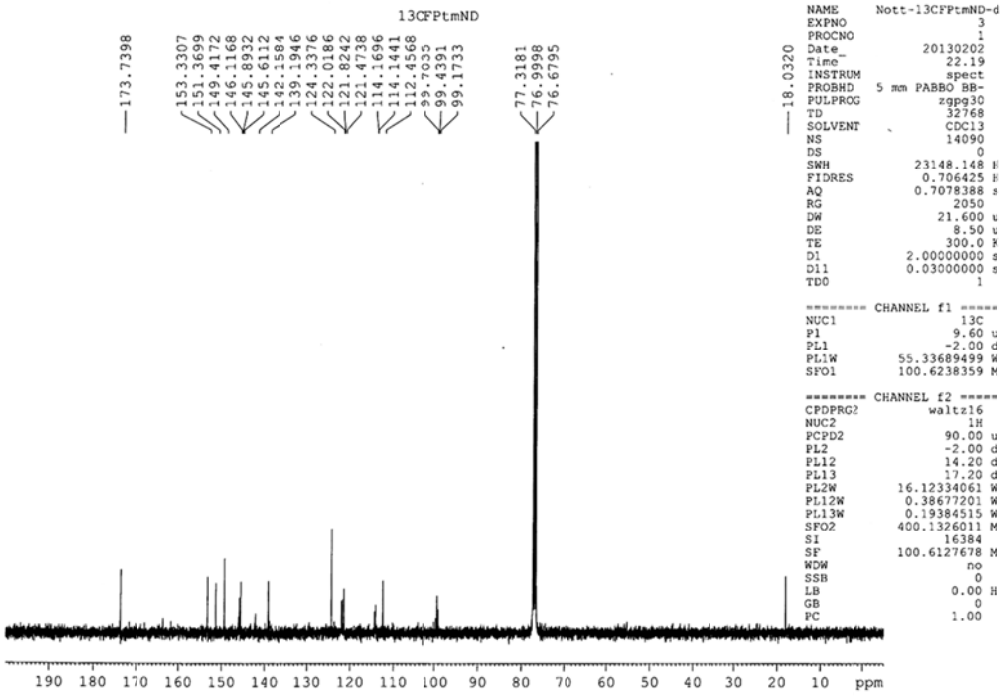

Figure S2 ^{13}C-NMR spectrum of **FPtmND.**

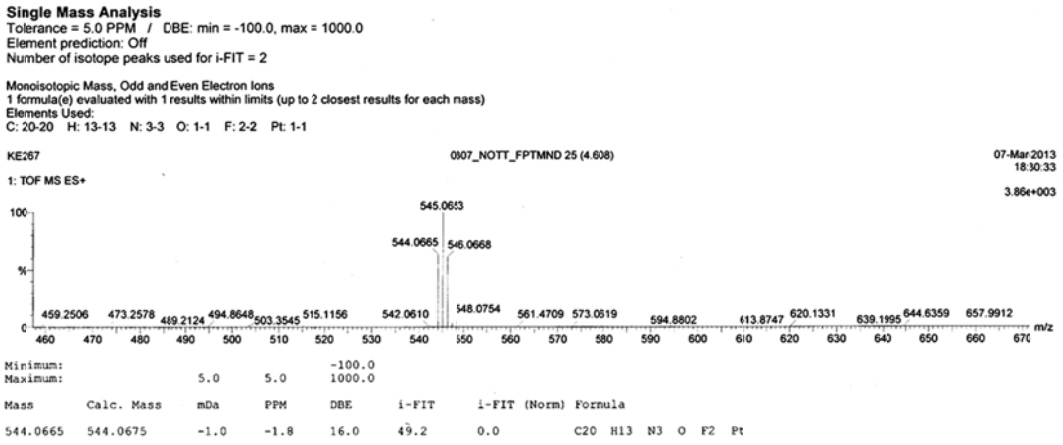

Figure S3 HR-ESI-MS spectrum of **FPtmND.**

Thermogravimetric analysis

The thermal stability of **FPtmND** was determined by using thermogravimetric analysis (TGA) under nitrogen atmosphere with a heating rate of 20 ^{o}C min^{-1}. A sample was heated up to 900 ^{o}C. No weight loss was observed in the range below 285 ^{o}C and the decomposition temperature, which is defined as a 5 wt% weight loss, appeared at 332 ^{o}C.

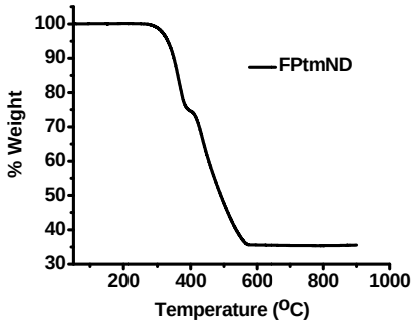

Figure S4 TGA thermogram of **FPtmND**.

Phosphorescence lifetime measurement

FPtmND dissolved in dichloromethane (1×10^{-5} M) was placed in a Schlenk cuvette. The sample solution was degassed according to freeze-pump-thaw procedure for 5 cycles. The phosphorescence emission was detected at 90^{o} via a second Czerny-Turner design monochromator onto a thermoelectrically cooled red-sensitive photomultiplier tube. The resulting photon counts were stored on a microprocessor-based multichannel analyzer. The instrument response function was profiled using a scatter solution and subsequently deconvoluted from the emission data to yield an undisturbed decay. Nonlinear least squares fitting of the decay curves (one

example is shown in Fig. S5) were performed with the Levenburg-Marquardt algorithm and implemented by the Edinburgh Instruments F900 software.

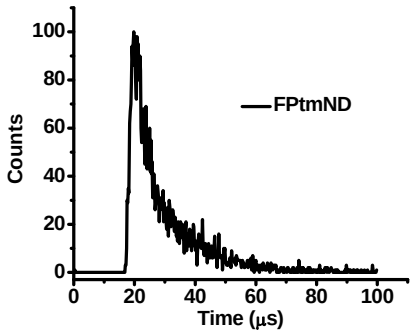

Figure S5 Excited decay profile of **FPtmND**.

Characterization of UV-visible absorption

The absorption spectra of **FPtmND** are displayed in Fig S6. **FPtmND** showed two major absorption bands. The strong absorption band at ≤ 300 nm are derived from π-π^* local transition of the ligands. The weak absorption bands around 300-450 nm have relatively small extinction coefficients and are assigned to transitions of mixed singlet metal-to-ligand charge transfer (^{1}MLCT) and triplet metal-to-ligand charge transfer (^{3}MLCT). Absorption spectra of thin film samples, which were prepared by solution-cast method, of NPB, **4P-NPD**, CBP, and TPBI were also recorded for the estimation of optical band-gap energy.

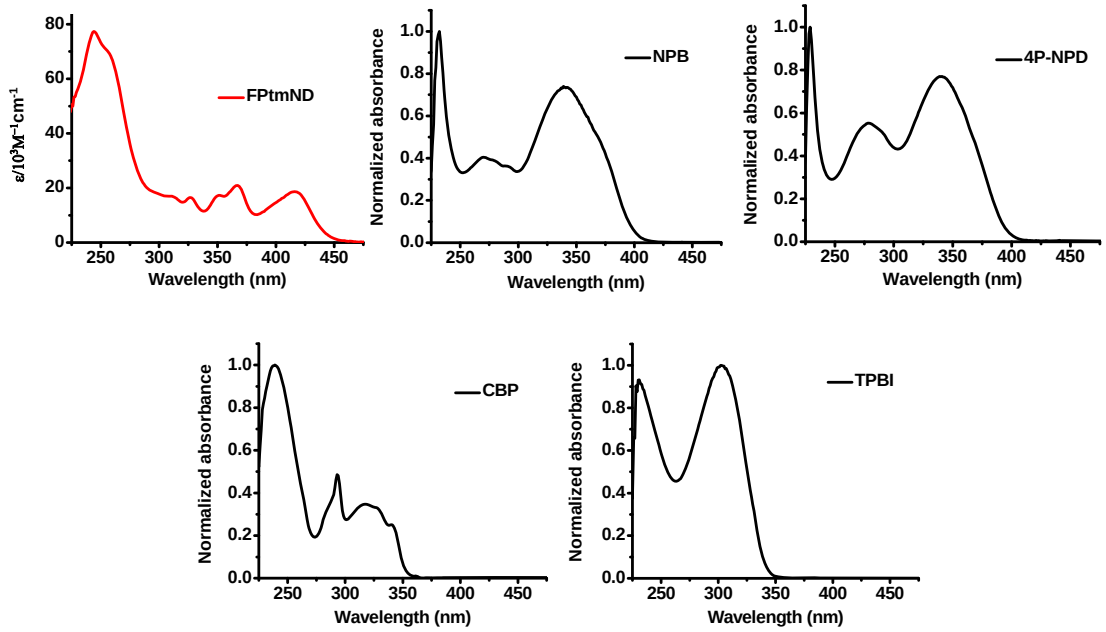

Figure S6 UV-visible absorption spectrum of **FPtmND** (1×10^{-5} M in CH_2Cl_2), thin films of NPB, **4P-NPD**, CBP, and TPBI.

Cyclic voltammetry and energy level determination

The energy level of HOMO was determined from the first electrochemical oxidation potential (*vs.* saturated $Ag/AgNO_3$), which is an average of the peak positions of cathodic and anodic current (Fig. S7). Energy level of ferrocene (4.8 V below the vacuum level) is used as the reference.[10] The HOMO energy levels were calculated with empirical relation $E_{HOMO} = -e[(E_{1/2}^{oxd} - E_{1/2(ferrocene)}) + 4.8]$ eV. The energy gaps (E_g) were determined from the onset wavelengths of the absorption spectra (Fig. S6). The LUMO energy levels were estimated by subtracting the energy gaps from the HOMO energy levels (Fig. S8 and Table S1).

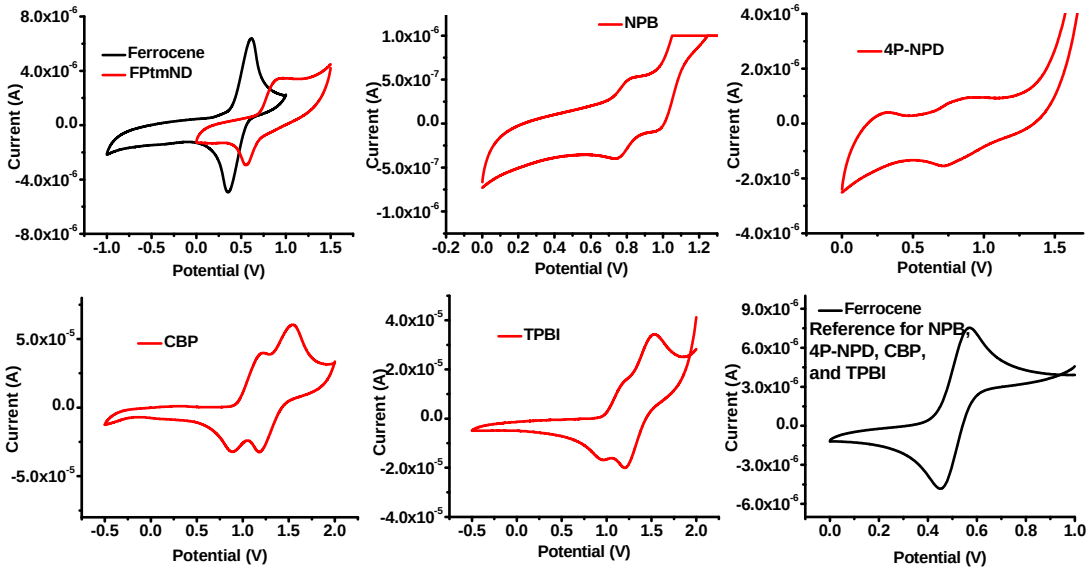

Figure S7 Cyclic voltammograms of **FPtmND**, NPB, 4P-NPD, CBP, TPBI, and ferrocene (reference).

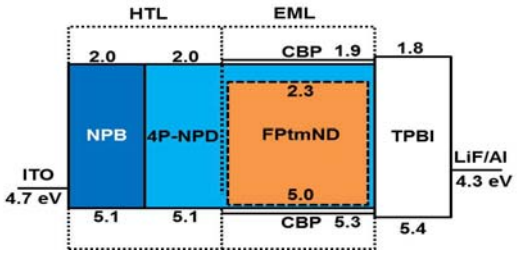

Figure S8 Energy level alignment of materials involved in OLEDs.

Table S1 HOMO and LUMO energy levels of **FPtmND** and organic materials

Complex	$E_{1/2}^{oxd,1}$ (V)[a]	E_{HOMO} (eV)	λ^{ab}_{onset} (nm)	E_g (eV)	E_{LUMO} (eV)
FPtmND	+0.71	5.03	448	2.78	2.25
NPB	+0.78	5.08	406	3.06	2.02
4P-NPD	+0.78	5.08	404	3.07	2.01
CBP	+1.03	5.33	358	3.47	1.86

TPBI	+1.06	5.36	346	3.59	1.77

Monitoring excimer/aggregate PL of FPtmND in thin film

A dichloromethane solution mixture containing FPtmND and either CBP or PS host was prepared. Such solution was dropwise applied onto quartz substrate. After solvent evaporation, thin film-coated quartz substrate was subjected to PL (Fig. S9) measurement by fluorescence spectrophotometer with 380 nm as the excitation wavelength.

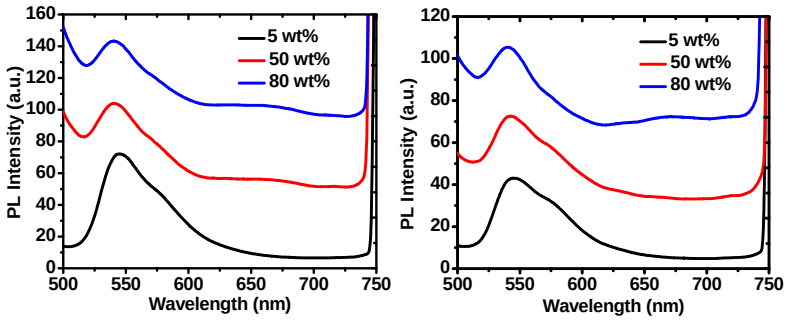

Figure S9 PL spectra (excitation wavelength 380 nm) of the thin film of FPtmND in CBP (left figure) and PS (right figure) hosted thin film. Each spectrum was off-set vertically for clarity.

Electroluminescence data

Table S2 Device performances with different doping concentrations.

Device	Conc. (wt%)	V_{on} (V)[a]	EQE (%)[b]	CE (cd A^{-1})[b]	PE (lm W^{-1})[b]	L (cd m^{-2})[c] voltage(V)	λ_{max}^{EL} (nm)	CIE (*x*,*y*)[d]	CRI[e]
A	2	4.5	8.6 9.1	31.3 32.6	14.5 15.7	15387 15	444 548	0.40 0.54	-
A	5	4.5	7.8 8.9	29.2 33.9	9.6 10.1	9153 15	548	0.42 0.56	-
A	8	4.5	7.5 7.6	28.6 28.8	11.8 16.17	25224 15	549	0.42 0.55	-
B	2	4.0	1.7 1.7	1.8 1.8	0.7 0.8	3211 15	442 604	0.18 0.12	-
B	5	3.5	4.2 4.3	5.6 5.8	2.9 3.1	8506 15	456 605	0.21 0.18	-
B	8	3.0	5.8 5.9	10.8 11.0	5.0 6.2	11188 15	443 603	0.39 0.29	83
B	50	4.0	9.4 9.5	7.4 7.5	3.3 4.8	23223 15	664	0.60 0.37	-
C	2	4.5	10.5 11.2	40.1 42.4	15.3 18.5	8596 15	548	0.38 0.57	-
C	5	3.5	14.2 15.1	57.0 58.3	21.4 26.1	16912 15	548	0.40 0.58	
C	8	5.0	9.1 9.7	32.3 34.2	10.2 16.6	9095 15	552	0.42 0.53	-
D	2	5.0	1.5 1.8	1.8 2.2	0.5 0.9	1077 14	446 603	0.20 0.16	-
D	5	3.5	6.0 6.1	10.9 11.3	4.7 6.7	7174 13	450 604	0.37 0.30	83
D	8	4	4.4 4.5	7.5 7.7	3.5 3.9	8589 15	450 616	0.55 0.39	-
D	50	4.5	8.9 9.0	9.3 9.6	3.3 4.1	12106 15	463 658	0.51 0.35	-
E	5	4	13.4 16.3	51.3 63.1	23.3 39.7	15226 15	546	0.40 0.57	
F	5	4.5	16.7 18.2	62.7 69.7	19.3 43.8	5234 15	552	0.42 0.56	-
G	5	5.0	9.2 9.3	24.0 24.1	7.2 9.6	4316 15	444 558	0.44 0.47	86
H	5	5.0	11.1 11.9	28.6 29.0	10.0 12.1	15119 15	442 572	0.41 0.41	89

[a] Turn-on voltage is the one at which the luminance over 1 cd m^{-2} was obtained; [b] The data for external quantum efficiency (EQE), current efficiency (CE), and power efficiency (PE) obtained at 500 cd/m^2. The data of peak efficiency is listed below each efficiency; [c]Maximum electroluminance (L) and voltage. [d]Commission Internationale d'Eclairage chromaticity coordinates at 8~9 V; [e] Color rendering index at 8~9 V.

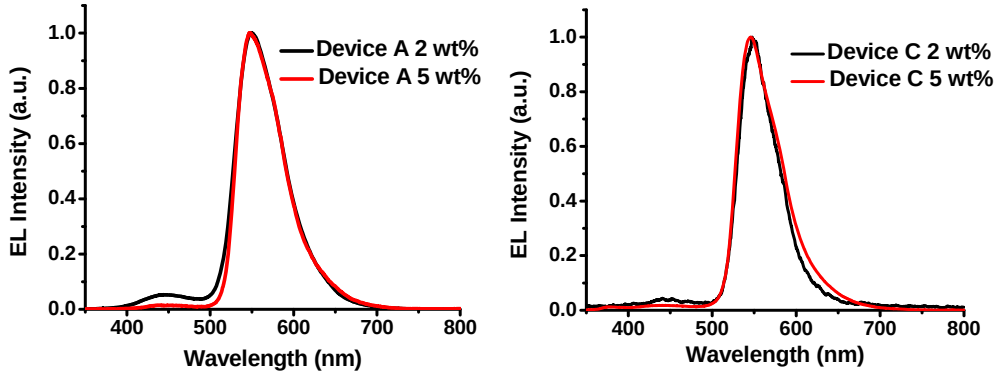

Figure S10 EL spectra of Device A and C with 2 and 5 wt% dopant concentration.

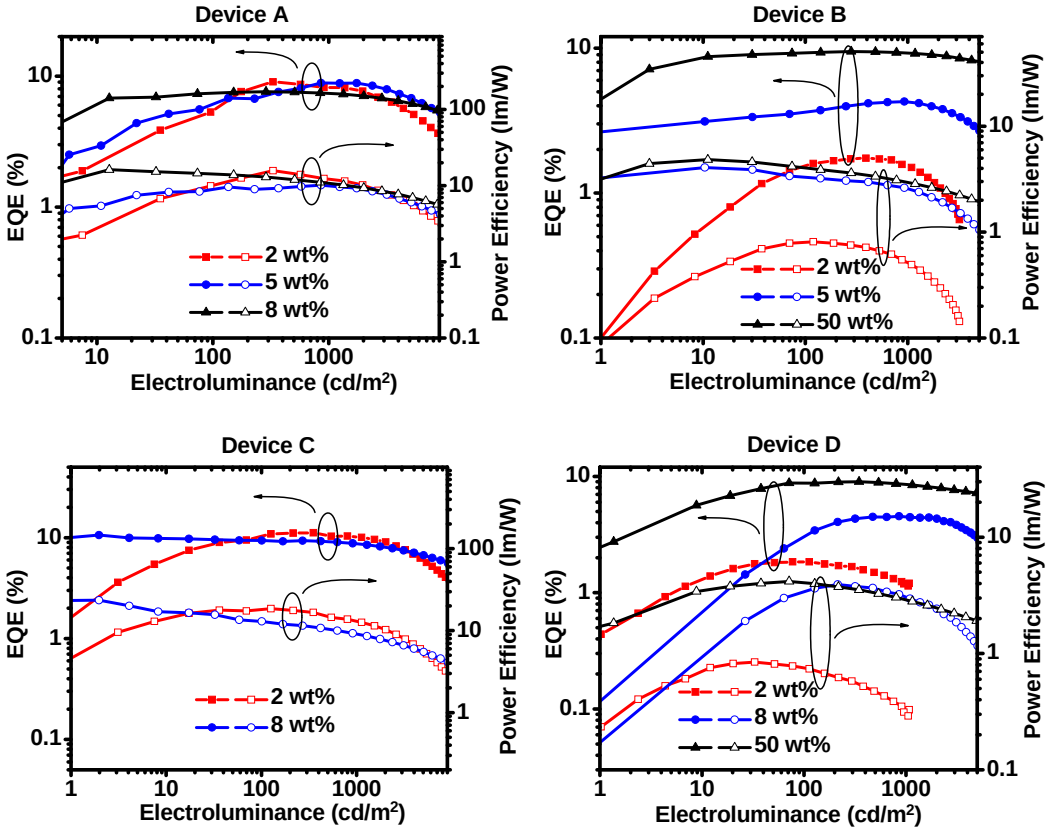

Figure S11 External quantum efficiency (EQE) and power efficiency as a function of electroluminance of Device A, B, C and D

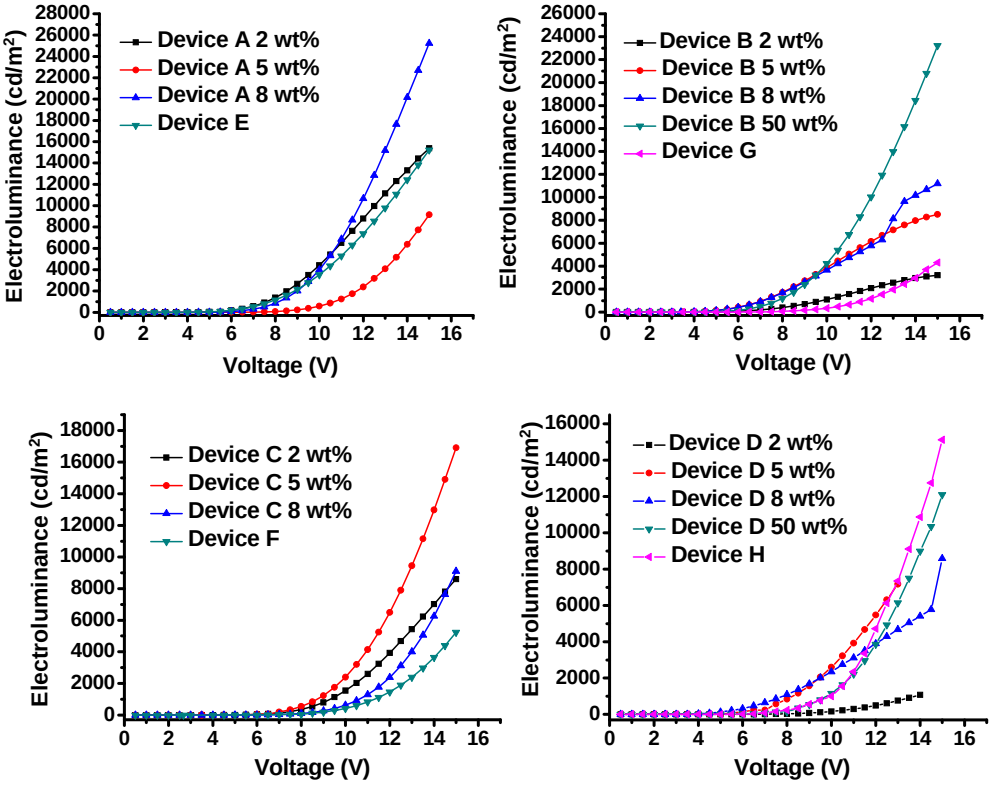

Figure S12 Luminance-voltage characteristics of Device A, B, C, D, E, F, G and H.

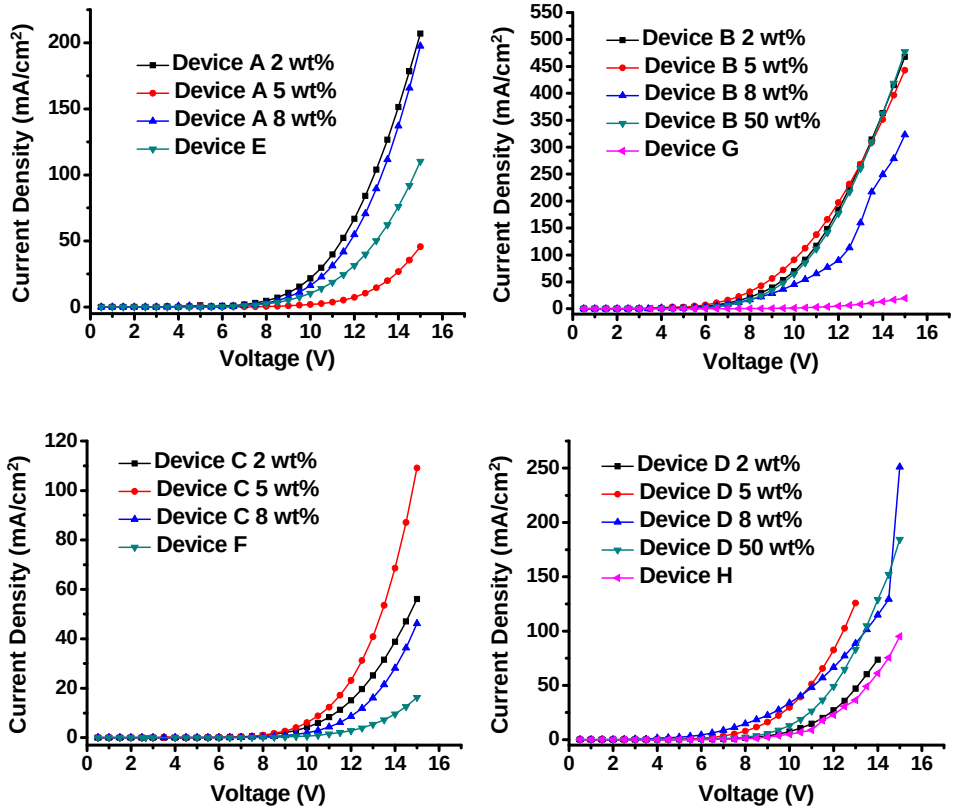

Figure S13 Current density-voltage characteristics of Device A, B, C, D, E, F, G and H.

References

1. B. E. Koene, D. E. Loy and M. E. Thompson, *Chem. Mater*., 1998, **10**, 2235.
2. P. J. Low, M. A. J. Paterson, D. S. Yufit, J. A. K. Howard, J. C. Cherryman, D. R. Tackley, R. Brookc and B. Brown, *J. Mater. Chem*., 2005, **15**, 2304.
3. Shi, J.; Tang, C. W.; Chen, C. H. U.S. Patent No. 5645948, 1997.
4. Y. You and S. Y. Park, *J. Am. Chem. Soc*., 2005, **127**, 12438.
5. S.-H. Liao, J.-R. Shiu, S.-W. Liu, S.-J. Yeh, Y.-H. Chen, C.-T. Chen, T. J. Chow and C.-I. Wu, *J. Am. Chem. Soc.*, 2009, **131**, 763.
6. H. Xu, K. Yin and W. Huang, *Chem. Eur. J*., 2007, **13**, 10281.
7. J. J. Michels, M. J. O'Connell, P. N. Taylor, J. S. Wilson, F. Cacialli and H. L. Anderson, *Chem. Eur. J*., 2003, **9**, 6167.
8. S. R. Forrest, D.D.C. Bradley and M. E. Thompson, *Adv. Mater.*, 2003, **15**, 1043.
9. J. Brooks, Y. Babayan, S. Lamansky, P. I. Djurovich, I. Tsyba, R. Bau and M. E. Thompson, *Inorg. Chem*., 2002, **41**, 3055.
10. M. Thelakkat, H.-W. Schmidt, *Adv. Mater*., 1998, **10**, 219.